

This document is published in:

Journal of the European Ceramic Society (2012). 32(16), 4063-4072.
DOI: <http://dx.doi.org/10.1016/j.jeurceramsoc.2012.06.023>

© 2012 Elsevier Ltd.

Torque rheology of zircon feedstocks for powder injection moulding

J. Hidalgo ^{a,*}, A. Jiménez-Morales ^{a,*}, J.M. Torralba ^{a,b,*}

^a Powder Technology Group of Department of Materials Science and Engineering of Carlos III University of Madrid, Leganés 28911, Spain
^b IMDEA Materials Institute, Madrid, Spain

*Corresponding authors at: Powder Technology Group of Department of Materials Science and Engineering of Carlos III University of Madrid, Av. Universidad 30, Leganés 28911, Spain. Tel.: +34 916249482.

E-mail addresses: jhidalgo@ing.uc3m.es (J. Hidalgo), toni@ing.uc3m.es (A. Jiménez-Morales), josemanuel.torralba@imdea.org (J.M. Torralba).

Abstract: In this work, a cellulose acetate butyrate (CAB) and polyethylene glycol (PEG) blend is used as the binder system in a zirconium silicate mineral powder feedstock for powder injection moulding. These irregular zircon powders make the mixing process and the selection of an optimal solid loading level a difficult task. Torque rheology methodologies combined with other techniques are used for evaluation of the parameters affecting the mixing process and determination of the critical powder volume concentration (CPVC). Temperature variations during the mixing process are monitored and used as an indicator of the friction energy of the system and thus for the optimal solid loading selection. There have thus far been limited amounts of work conducted on torque rheology of highly loaded feedstocks that incorporate a study of the system's temperature evolution. A detailed study could be a key factor for understanding the mixing behaviour of highly loaded feedstocks.

Keywords: Injection moulding; Rheology; Zircon

1. Introduction

Powder injection moulding (PIM) has become a competitive manufacturing technology that can be applied to nearly any ceramic or metallic material processed as fine powder. PIM is suitable for applications which require a large production series of complex geometries, even to the point of occasionally being the only viable method for producing a particular part or product.

The solid loading level and mixing methods are two factors that determine many characteristics of the feedstock. Feedstock homogeneity during the mixing stage is crucial to achieving good results throughout the PIM process and consistent products.^{1,2} Careful choice of mixing method and parameters is the key for achieving a homogeneous mixture that is free of agglomerates and has an optimal powder and binder content.³ Solid loading is defined as the ratio of powder volume to the total volume of solids and binder. Determination of the optimal solid loading admitted by the binder system is also important. After binder removal, much empty space is left between powder particles, which should be filled by atomic diffusion during the sintering stage. This mass transfer during sintering causes shrinkage and densification in the piece. Minimising the binder

content without compromising the rheology and the integrity of the feedstock assists in increasing process tolerances and reducing cycle time.

Torque rheometers are used extensively as tools for characterising the evolution of the feedstock component mixing process and for evaluating the mixture homogeneity. They have also been demonstrated to be quite useful for determining the optimal and critical solid loadings for a feedstock.^{4,5} In a torque rheometer, the torque exerted by gyratory rotors to displace a bulk of a fluidised mass is measured as a function of the time to create a plot of torque vs. time, called a rheogram. The torque is related to the fluid viscosity and can thus serve as a measure of the resistance of a fluid to deformation by either shear or tensile stress.⁶

In this work, torque rheology was used to characterise some important aspects of the mixing behaviour of micron-size zircon powders with water soluble binder systems based on PEG and CAB. Variations in mixing torque and feedstock temperature over time at several different solid loading levels has been studied. Zircon powders have non-conventional attributes for a PIM process which requires special consideration for the interpretation of results. Several authors have noted atypical behaviour in

torque-based evaluations of the critical powder volume concentration (CPVC) of non-conventional PIM powders. Aggarwal et al.⁷ describe abnormal rheological behaviour in torque experiments to determine the critical solid loading of irregularly shaped niobium powders. The CPVC value could not be clarified with this method due to absence of instabilities for solid loading values in the CPVC region. Barreiros et al.⁸ also note the problem and further present a new methodology for the determination of critical solid loading by torque rheology for unconventional PIM powders, based on the intersection of different linear trends in plots of torque vs. solid loading.

These non-classical torque behaviours make it difficult to determine the feedstock's critical solid loading. Feedstock temperature will be monitored during mixing, which will reveal some important aspects to consider when the critical solid loading is assessed. Although it is well known that temperature influences rheology, its variation during the mixing process is not often⁹ considered in torque rheology. For supporting torque rheology measurements, capillary rheology and density measurements of the resulting feedstock have been carried out. A complete PIM process has been also carried out for a feedstock composition optimised with the above methodologies proposed.

2. Materials

Micronised mineral zirconium silicate sand was used for the study. The powders were supplied by GUZMAN GLOBAL S.L (Nules, Spain). They present an irregularly shaped morphology as shown in Fig. 1, which also shows the particle size distribution curves for the zircon powder. A Malvern 2000 laser scattering particle size analyzer was used to measure particle size distribution. The irregular morphology of these powders contrasts with the spherical or round-shaped powders conventionally used for PIM.

The particle size of the D₅₀ and D₉₀ powders are 1.604 and 4.65 μm, respectively, which corresponds to values extremely low for PIM. The powders have a specific surface area of 5.0363 m²/g, which was measured using a Micrometrics Gemini VII BET measurement device. The low tap and apparent densities, 32.45% and 21.07% of the material density (4.58 g cm⁻³), respectively, reflect the low packing capacity of the powders and their tendency to form agglomerates, both of which are a direct consequence of the unconventional shape of the powder. These unattractive characteristics would normally make the powder unsuitable for a PIM process.² PIM has generally been limited to high performance and dimensionally precise components, associated with the use of expensive raw materials with tailored characteristics. The use of non-conventional PIM powders such as natural raw materials or waste products from other processes has been investigated and shown to be possible.^{10,11} This previous work leads us to consider the use of as-supplied natural zircon mineral sand as a possible raw material for PIM purposes.

A binder system based on polyethylene glycol (PEG) and cellulose acetate butyrate (CAB) was selected. This type of binder has been demonstrated to be effective for zircon PIM, providing improved properties compared with other binder systems.¹² Two

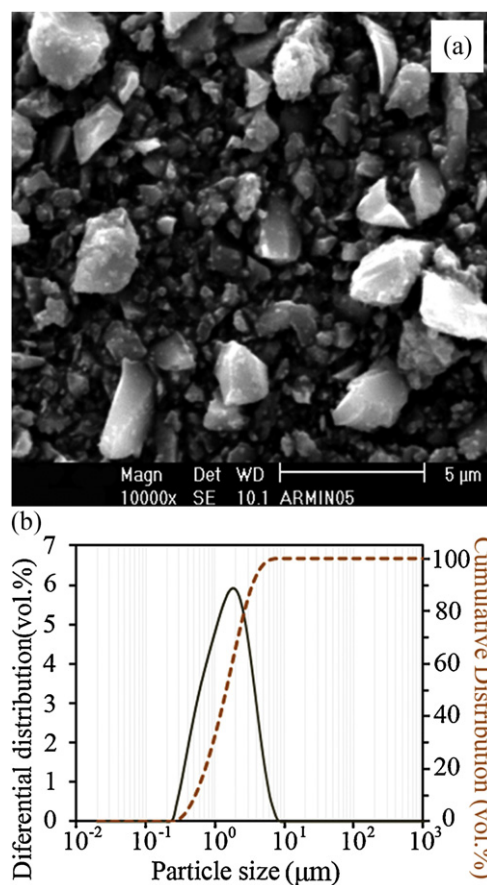


Fig. 1. (a) An SEM micrograph of zircon powders and (b) their particle size distribution curves by laser scattering.

types of CAB, CAB381-0.1 and CAB551-0.01, with different percentages of butyryl, acetyl and hydroxyl groups were blended with two types of PEG, PEG20K and PEG4K, with different average molecular weights. The composition of the binder system and the characteristics of the components are summarised in Table 1.

3. Experimental procedure

A Rheomix 600 Haake rheometer coupled with a Haake Rheocord 252p module equipped with roller blade-type rotors was used to perform the mixing experiments. A temperature of 150 °C and a rotor speed of 50 rpm were used in all experiments and the mixing chamber was filled up with feedstock to 72% of its volume (the total chamber volume is 69 cm³). Feedstock temperature and torque were monitored as the output

Table 1
Composition of the binder.

	CAB381-0.1	CAB551-0.01	PEG20K	PEG4K
vol.%	10	30	58	2
T _{MELT} (°C)	155–165	127–142	63–66	58–61
T _{GLASS} (°C)	123	85	<0	<0
M _w	20,000	16,000	20,000	4000
Supplier	Eastman	Eastman	Aldrich	Aldrich

parameters. The equipment is self-calibrating as it reloads at a start of every new measurement. A thermocouple is placed at the confluence of the rotors' flow, where the feedstock is well-mixed, to monitor the temperature of the feedstock. A value for the critical solid loading or critical powder volume concentration (CPVC) will be determined by experiments varying the solid loadings. The CPVC is the ratio at which powder particles are tightly packed and binder fills all the voids between particles. In previous experiments, results have been demonstrated to be highly sensitive to the way in which components are added as well as the percentage of the mixing chamber occupied by the feedstock. Zircon powders, CAB powders and PEG flakes are first mixed and homogenised with a Turbula mixer at room temperature for 1 h, and then poured into the rheometer together. The as-prepared solidified feedstocks were grinded in a blade mill to create pellets for further experiments of density measurements and capillary rheology.

To complement torque results, capillary rheology was carried out in a Bohlin Instruments RH2000 Capillary Rheometer. The study comprises the investigation of the relationships between the viscosity and: (1) the shear rate (in a range from 10 to 10,000 l s^{-1}), (2) temperature (trials from 140 to 170 $^{\circ}\text{C}$ each 10 $^{\circ}\text{C}$) and (3) solid loading. Several dies and transducer pressure sensors were used to allow a wide shear rate range (3 magnitude orders) and pressure range with the maximum accuracy possible and attending the interval of solid loading proposed. The relation between the die diameter and its length was kept constant in a value of 30, which is the minimum recommended to achieve a laminar flow along the die. In all the cases the apparent shear viscosity was calculated.

4. Results

4.1. Critical solid loading by torque rheology

In Fig. 2, torque vs. time rheographs and temperature vs. time curves are presented for different solid loadings ranging from 52.5 to 65 vol.%. The mixing time was fixed at approximately 50 min. For low solid loading contents (52.5, 55 and 57.5 vol.%), the torque value stabilises relatively quickly, in less than 30 min from closure of the internal mixing chamber (this corresponds approximately to the maximum torque value registered for each experiment). For the remainder of the higher solid loading content samples, stabilisation of the torque is not completely achieved within 50 min. The feedstock temperatures measured during the experiments also follow this trend.

The temperature vs. time curves appears to follow similar trends as those of torque vs. time. The evolution of both parameters, in the case of high polymer loading, can be explained mainly as a direct consequence of the interparticle friction. Thus, both parameters evolve similarly as the particles come closer together with increased solid loading. The only deviation from this trend occurs during the first stage of mixing, but can most likely be attributed to increased temperature from the heating plates rather than particle friction.

Monitoring the temperature can be a helpful complementary tool to find the optimal and critical solid loadings. The critical

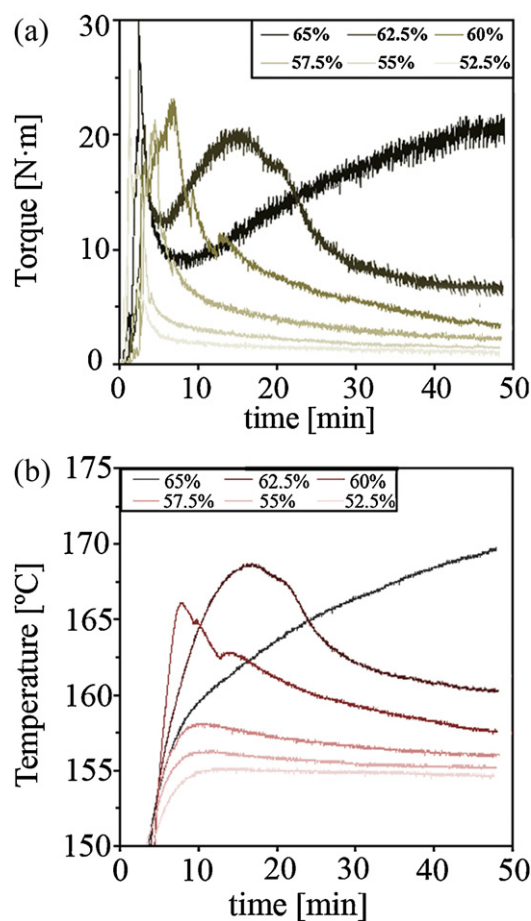


Fig. 2. (a) Torque vs. time and (b) temperature vs. time curves for several solid loading expressed vol.%.

solid loading could be determined as 65 vol.% because torque and temperature do not stabilise even after a long period of time. The temperature exceeds 170 $^{\circ}\text{C}$, which is 20 $^{\circ}\text{C}$ above the programmed mixing temperature. However, the 62.5 vol.% sample also shows severe difficulty in achieving equilibrium and high temperatures during the mixing process, indicating high interparticle friction. Furthermore, for both solid loading values, the average difference between consecutive registered torque values is higher than for the rest of the solid loadings, an indicator of composition heterogeneities and a solid loading over the critical value. This controversy highlights the necessity of employing complementary characterisation techniques to come to a clear conclusion.

The area under the torque vs. time curve at a given time is commonly referred as totalised torque (TTQ).¹³ This value, which represents the energy being put into the system during that given time, is also representative of the total energy dissipation rate in a suspension or likewise, in loaded polymeric blends. TTQ can be used to estimate the relative network strength in suspensions,¹⁴ or the processability of polymer-filler composites.¹⁵ In this work, TTQ is proposed as an estimate of friction energy because binders are highly loaded and friction forces predominate over cohesion forces. The TTQ values could also be converted to work energy by equations found in

Table 2
Processability parameters after 50 min of mixing.

Powder (vol.%)	M (N m)	ΔM (N m)	T ($^{\circ}\text{C}$)	TTQ (J min)	E_t (kJ)	E_{sp} (J/g)
52.5	1.06	0.18	154.8	99.7	31.3	213.0
55	1.44	0.14	155.2	129.7	40.7	269.5
57.5	2.20	0.30	156.0	202.1	63.5	408.9
60	3.18	0.26	157.4	376.7	118.3	742.4
62.5	6.15	0.48	160.8	579.9	182.2	1114.1
65	20.20	0.98	169.3	738.3	231.9	1383.6

the literature.^{14,16} The work energy supplied to the system by the rotors (E_t) represents a force (F) multiplied by a distance (d). In a torque rheometer, the distance covered by the blade is equal to the angular speed (N) expressed in rpm, multiplied by the average blade radius (r) and by two times pi. Considering that torque (M) is a function of force, $M = F \cdot r$, the work energy as a function of TTQ is reflected in expression (1):

$$E_t = F \cdot d = 2 \cdot \pi \cdot r \cdot N \cdot \int_{t_1}^{t_2} \left(\frac{M(t)}{r} \right) \cdot dt$$

$$= 2 \cdot \pi \cdot N \cdot \text{TTQ} \quad (1)$$

The specific energy of processing (E_{sp}) is obtained from E_t as a function of the material mass inside the mixing chamber (Eq. (2)),

$$E_{sp} = E_t \cdot m_{\text{feed}}^{-1} \quad (2)$$

The percentage of specific energy dissipated by friction can be assessed considering the overheating of the feedstock together with the specific heat of the feedstock (Eq. (3)),

$$E_{\text{frict}} = c_{\text{feed}} \cdot \Delta T_{\text{oh}} \quad (3)$$

To better interpret the torque results, totalised torque curves are presented for the different solid loading levels in Fig. 3. Processability parameters are summarised in Table 2. The value M represents the average torque value across the torque stabilisation region. Then the ΔM parameter represents the average deviation of the torque values from the average value for this

region and is a rough indicative of the feedstock homogenisation; the lower the ΔM the better the homogenisation.

It should be noted that all totalised torque curves have approximately the same slope at the first stages of the experiment. This indicates that in all cases, approximately the same amount of energy is dissipated per unit of time during this period. This result is consistent if it is considered that at the very beginning, all mixtures are in a similar situation in which interparticle friction is predominant before complete particle dispersion in the binder. This slope is maintained for a period of time depending on the solid loading level, and then it changes to a less pronounced slope which is maintained for the rest of the experiment.

The period in which the initial slope is maintained depends on the ability of the system to incorporate the binder and coat the particles. The ability of the system to accomplish it decreases as the solid content increases. The final slope also rises as the solid loading increases, which indicates the increasing dissipation of energy and is also consistent with the increased temperature behaviour. As the solid loading increases, less binder is available to lubricate the particles, decreasing inter-particle distance and increasing the probability of contact. Friction work is converted into heat. As the friction work increases, the system is less able to dissipate heat and thus, the temperature rises. All the materials behave following curves that, after an initial period of strong growing, tend to reach a steady state regime with the time, except those curves for 62.5 and 65%. In these former cases, the curve for 62.5% seems to be capable to reach the steady state regime after much higher times, but the curve related 65% it cannot be occur. This behaviour could be an indicator that the CPVC has been reached or overcome.

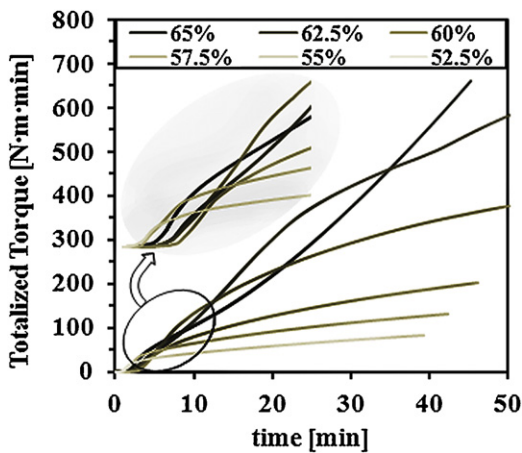


Fig. 3. Totalised torque curves for different solid loadings in vol.%.

4.2. Feedstock density measurements

Determination of the CPVC was also accomplished with a density technique. The density of the resulting solidified feedstock was measured with a Micrometrics AccuPyc 1330 helium pycnometer. For compositions above the critical solid loading, the amount of binder is insufficient to cover the particles and fill the remaining free volume. This results in the formation of voids inside the feedstock bulk; considering that no material is lost during the mixing process, this means that the density will be lower than the theoretical density. Determination of the CPVC by measurement of the feedstock density takes this fact into account. For solid loadings near 100 vol.%, voids begin to interconnect creating an open porosity and the density values begin to approach the theoretical ones once again.

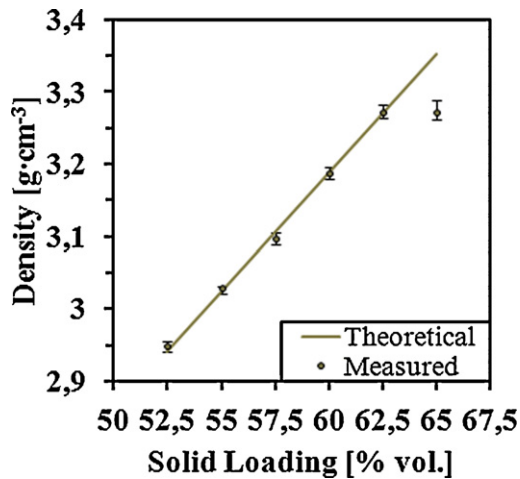


Fig. 4. Density (theoretical and measured) of the feedstocks for different solid loadings.

The density values for the different feedstocks are shown in Fig. 4. It can be appreciated that for all the different solid loading levels, the measured value is very close to the theoretical value. Moreover, the deviation of the measured density values from a mean density calculated from three different batches is almost negligible. The only exception is the 65 vol.% solid loading sample; the pronounced divergence from the theoretical density indicates excess powder content and the resulting formation of voids. This observation, taken together with the torque experimental results, indicates that the critical solid loading value is approximately 62.5 vol.%. The formation of voids can be observed in Fig. 5, which shows scanning electron microscope (SEM) images of as-prepared 52.5 and 65 vol.% solid loading feedstocks. In the 52.5 vol.% solid loading sample, shown in Fig. 12A, it can be observed that the binder completely covers all powder particles, representing an excess of binder. For the 65 vol.% solid loading feedstock shown in Fig. 12B there are heterogeneous regions indicating a lack of binder and voids are clearly visible.

4.3. Capillary rheology

Capillary rheology was used both to determine the rheological behaviour of the feedstocks and to assess the CPVC value. This kind of rheology allows studying the viscosity and its dependence with different affecting variables. The main influencing variables on the viscosity of PIM feedstocks, shear rate ($\dot{\gamma}$), temperature (T) and solid loadings (ϕ), were analysed.

4.3.1. Shear rate and solid loading viscosity dependence

Regarding the shear rate viscosity dependence, PIM feedstocks normally behave as pseudoplastic materials along the entire shear rate ranges typical for PIM (10^1 – 10^4 s⁻¹); their viscosity decreases with an increment of shear rate. This behaviour can be approximately described by the power law (4):

$$\eta = k \cdot \dot{\gamma}^{n-1} \quad (4)$$

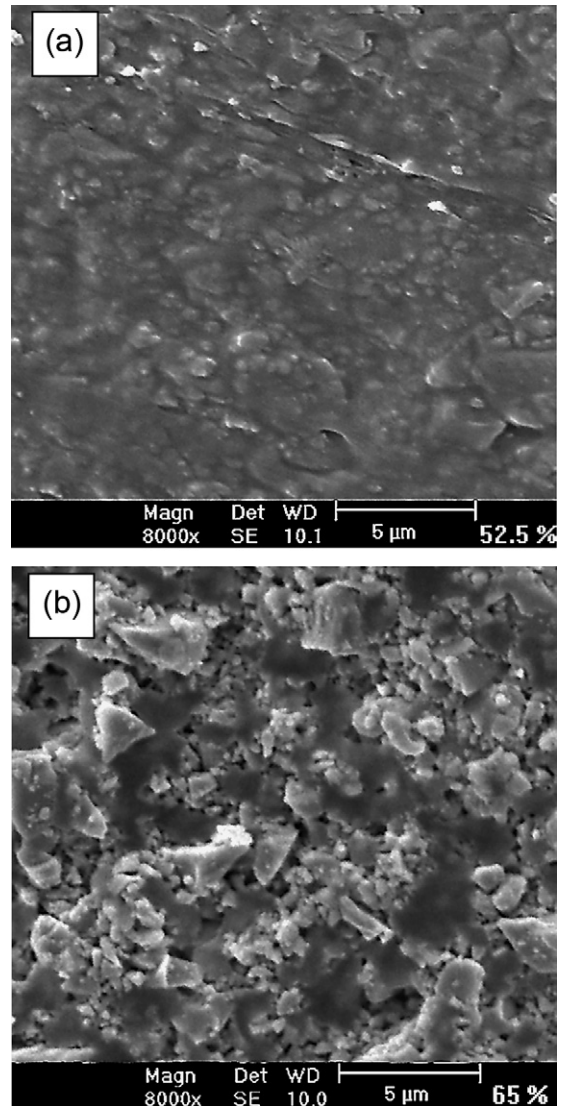


Fig. 5. SEM images of as-prepared feedstocks: (a) 52.5 vol.% of zircon, (b) 65 vol.% of zircon.

where n is the so-called flow index and represents the shear rate sensitivity. Values of $n < 1$ corresponds to the mentioned pseudo-plastic behaviour. As the value approaches $n = 1$ the feedstocks viscosity becomes less sensitive to shear rate until the value 1 is reached; in that case viscosity does not depend on shear rate. This kind of behaviour is referred as Newtonian. For values higher than 1, viscosity increase with an increment of shear rate which is referred as dilatant behaviour. Powder law is effective for its straightforwardness, but fails in predicting viscosity when shear rate trends to zero or infinite. It requires materials with infinite viscosity at shear rates near zero and zero viscosity as the shear rate take values near infinite which is not the common case. There are a number of other models that could better describe the whole flow behaviour of shear-dependent fluids, but they do so at the cost of simplicity.

Fig. 6 shows the variations of the shear viscosity value for different shear rates in the range from 10^1 to 10^4 s⁻¹ and for the temperature of 160 °C. In low solid loading feedstocks (52.5 and 55 vol.%) a Newtonian behaviour is distinguished for low shear

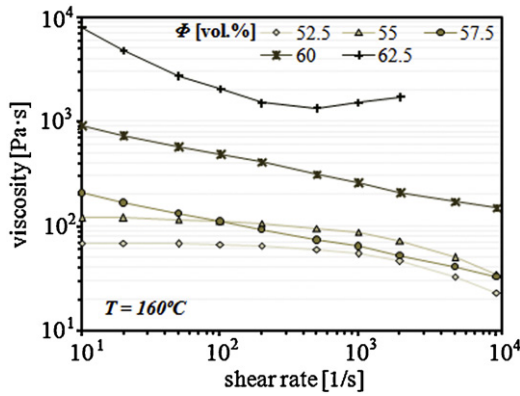


Fig. 6. Experimental results of the shear viscosity dependence with shear rate for different percentages of solid loadings for 160 °C.

rates, which turns into pseudoplastic for higher values. This fact happens for all the temperatures studied (from 140 °C to 170 °C), being markedly more clear at higher temperatures. The turning point for the behaviour change is displaced to lower shear rate values as the temperature decreases. For 57.5 and 60 vol.%, the behaviour is completely pseudoplastic. In case of 57.5 it can be seen at Fig. 6 that the curve overlaps the 55 vol.% one. This is an uncommon behaviour as it is a generally accepted statement that viscosity of compounds at all concentrations is higher than of the preceding lower concentration.

An explanation is unclear, but it could be justified considering the presence of agglomerates. Torque rheometer could be limited for exerting enough shear stresses to agglomerate breakage.³ If the binder is not able to provide with enough shear stress too, high binder contents could also limit agglomerate breakage.¹⁷ However during mixing process of high solid loadings concentrations at torque rheometer, agglomerates interactions increase. Thereby erosive effects become notorious and thus it does agglomerate rupture. It is well established that presence of agglomerates affects feedstock viscosity; the greater the number of particles in the agglomerate, the lower the packing density and the higher viscosity.^{1,2} This should also be reflected accordingly in the torque values, but stabilised torque values increase with the solid loading. Nevertheless, the shear rates in torque rheometer are in the order of 10–100 s⁻¹.⁶ For such values, capillary rheology results are consistent with torque measurements. In contrast, shear stresses produced by the capillary could be high enough for develop hydrodynamic or erosive agglomerates destruction at high shear rates. It is widely accepted that the change from Newtonian plateau to non-Newtonian flow arises from the disruption of agglomerates¹⁸ among other possible factors, which would explain the behaviour observed. As the experiment temperature is increased, viscosity of binder decreases as well as the viscous forces imposed by the binder on the particles making the agglomerated structure to prevail for a wider shear rate interval.

In the case of 62.5 vol.% feedstock, a dilatant behaviour is observed for high shear rates. This is an indicative that a solid loading percentage is within the region near the CPVC and the feedstock is not suitable to be injected. Moreover, pressures registered for values above 2000 s⁻¹ exceed the maximum of the permitted by the pressure transducer used. The same occurs

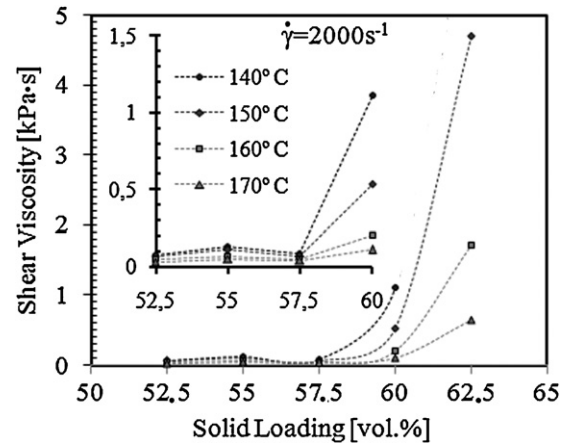


Fig. 7. Dependence of shear viscosity with solid loading for different temperatures and for the shear rate of 2000 s⁻¹.

with 65 vol.% of solid loading in which no viscosity value could be registered for any temperature value, being imprecise if this happened because of flow restriction or equipment limits.

The solid loading dependence of viscosity for different temperatures at 2000 s⁻¹ is shown in Fig. 7. There it could be appreciated more clearly the viscosity fall from 55 to 57.5 vol.% that come about for all temperatures and then the abrupt rising for higher solid loadings. At critical solids loading the feedstock has a very high viscosity therefore slight excess binder is used to provide lubricity for moulding, thereby, solid loadings of 60 and 62.5 vol.% seems to approach or meet the CPVC condition. It looks like the mixing process of 57.5 vol.% was more effective in the rupture of agglomerates and getting all the components together, therefore, the viscosity descend due to a better packing. However, excepting 62.5 vol.%, all the feedstocks present viscosities under 10³ Pa s for all the shear rates and for temperatures above 150 °C. These values are considered quite reasonable in PIM processes for making possible proper mould filling.

4.3.2. Temperature viscosity dependence

The study of the dependence of feedstock viscosity with the temperature is also important. If the viscosity is very sensitive to the temperature variation, any small fluctuation of temperature during moulding will produce viscosity changes, producing stress concentration in the moulded part, resulting in cracking and distortion. The influence of temperature on viscosity can be expressed by the Arrhenius type Eq. (5):

$$\eta = B \cdot \exp\left(\frac{E_a}{R \cdot T}\right) \quad (5)$$

where E_a represents the activation energy, R is the gas constant and B is the viscosity at the reference temperature T_0 . Fig. 8 shows the temperature dependence of viscosity results for 57.5 vol.% at different shear rates. The activation energy at a certain shear rate and the reference parameter may be estimated by plotting the neperian logarithmic of viscosity of feedstock against the inverse of temperature. The E/R coefficient represents the slope of the resulting linearisation curve.

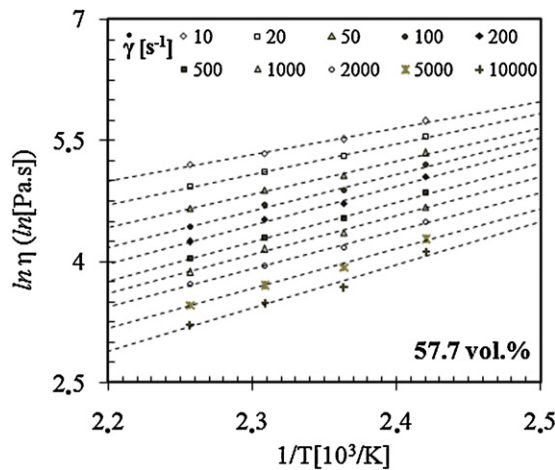


Fig. 8. Dependence of shear viscosity with temperature for solid loading of 57.5 vol.%.

Table 3 collects values of activation energies for different solid loadings and shear rates. Allaire et al.¹⁹ proposed the activation energy value of 40 kJ/mol as the level above which the probability of defects occurring during injection moulding becomes unacceptable for sub-micrometer zirconia blends. All the activation energies, except for the 57.5 vol.% of solid loadings, fairly exceeds this value in almost all the shear rates. These deviations are more pronounced at high solid loadings. In that cases, activation energy increase with the shear rate. For lower solid loading this tendency is the inverse. The reduction of viscosity owing to the pseudoplastic behaviour of these feedstocks at high shear rates appears to dominate the changes in viscosity related to temperature.

4.3.3. CPVC determination

The graph presented in Fig. 9 shows the evolution of n , B and E rheology parameters with variations of solid loadings for the reference conditions of 160 °C and 2000 s⁻¹. A region of pronounced sudden variation of all rheological parameters (n , E , and B) occurs at 57.5–60 vol.% solids loading. This region can be considered as critical solids loading region. A minimum activation energy is obtained for the 57.5 vol.%, being this solid loading the less sensitive to temperature variations. This minimum marches with a maximum of the B parameter and an inflection point in the value of the flow index. These indicators have been used in several works to give clues of the CPVC values (see Fig. 10).^{4,7}

Table 3
Values of the activation energy for different solid loadings and shear rates.

Φ (vol.%)	$\dot{\gamma}$ (s ⁻¹)			E_a (kJ/mol)
	20	200	2000	
52.5	79.49	64.24	52.32	
55	76.40	59.84	46.61	
57.5	44.54	40.02	35.90	
60	106.66	119.55	119.65	
62.5	97.75	252.18	153.72	

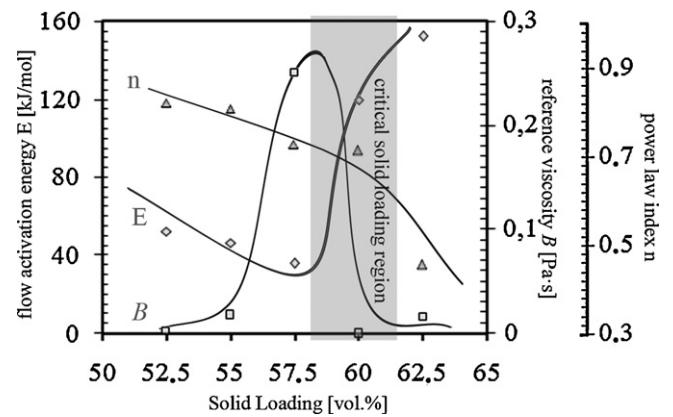


Fig. 9. Determination of the solid loading region.

4.3.4. General moldability parameter

In the above paragraphs rheology parameters were separately studied and plotted in different axes giving unclear or incomplete insights for optimal solid loading value determination. A general moldability index α_{stv} is proposed to summarise and globally describe the rheological behaviour of a feedstock taking into account all the parameters. This index was developed to compare the moulding capacity of plastics,²⁰ but its utility for other different systems like PIM feedstocks has being also contrasted.²¹ The subscripts s , t , v represents the shear sensitivity, temperature sensitivity and viscosity respectively. The general moldability index is defined as (6):

$$\alpha_{stv} = \frac{1}{\eta_0} \cdot \frac{|((\partial \log \eta)/(\partial \log \dot{\gamma}))|}{((\partial \ln \eta)/\partial(1/\tau))} = \frac{1}{\eta_0} \cdot \frac{1-n}{E/R} \quad (6)$$

where η_0 in this work was taken as the reference viscosity at 160 °C and shear rate of 2000 s⁻¹. The n parameter is the power law flow index and it was calculated by linearisation of power law at the pseudoplastic region of the curves. Linearisation was carried out by taking logarithms in both sides of Eq. (4).

The higher the moldability index is the better the general rheological properties are. In that respect it can be stated that 57.5 vol.% feedstock presents the most favourable rheological

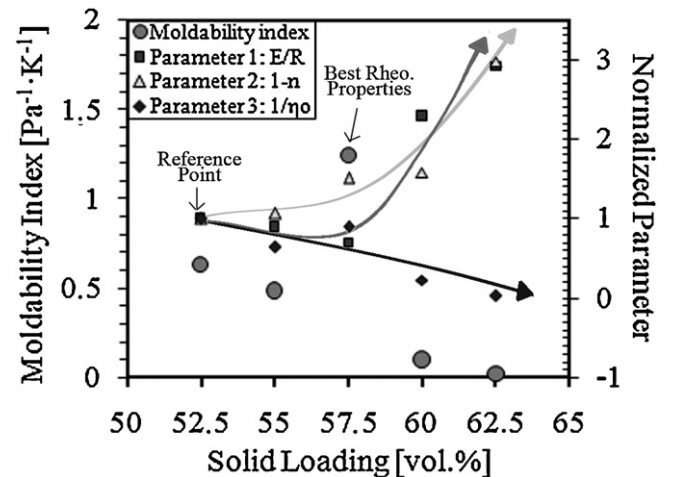


Fig. 10. General moldability index vs. solid loading vol.%.

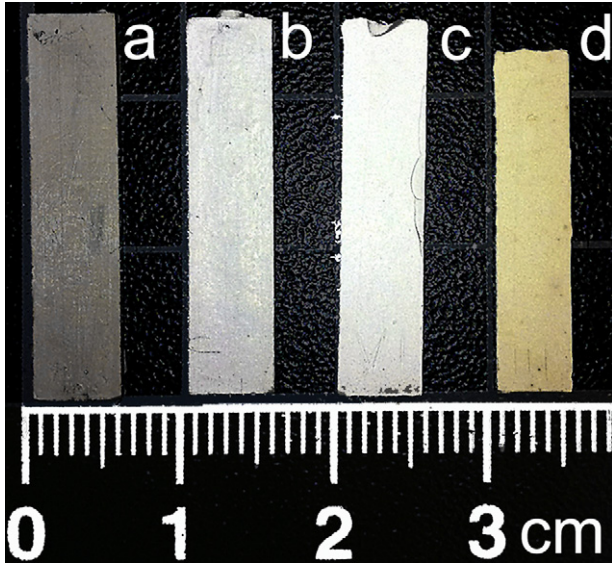


Fig. 11. Evolution of specimens during the different stages of the PIM process: (a) injected green part, (b) brown part after solvent debinding, (c) brown part after thermal debinding and (d) sintered part. (For interpretation of the references to colour in this figure legend, the reader is referred to the web version of this article.)

characteristics, therefore, it can be considered as the optimal solid loading. This solid loading presents the higher value of the moldability index resulting from balanced values of the parameters $1/\eta_0$, $1 - n$ and E/R which evolve differently with solid loadings.

4.4. PIM of optimal solid loading feedstock

A whole PIM process was carried out for 57.5 vol.% feedstock. Bending test specimens with dimensions, 25.2 mm large, 5.61 mm wide, 0.94 mm thick, were injected in an ARBURG injection moulding machine. Temperature of 150 °C and pressures of 1800 bar produces best densified green parts out of flaws. Two steps binder removal was carried out. First, a solvent debinding in water was performed to remove PEG and create open channel to facilitate further CAB thermal elimination without defects formation. At 60 °C, 86.76 vol.% of PEG was removed in 2 h. A thermal debinding in air up to 550 °C allowed burning out completely all the remaining CAB as registered in thermo-gravimetric analysis measurements with a Perkin Elmer STA6000. The sintering process consisted on a two step sintering cycle in air. Brown specimens were heated up to 1400 °C holding this temperature for 15 min. Then they were cooled until reach 1100 °C; this temperature was maintained during 120 min before cooling to room temperature.

In Fig. 11 pieces after different stages of the PIM process are presented. The evolution of the specimens' dimensions could be observed. Globally, after sintering, a volumetric shrinkage of 24.82 vol.% was achieved. Pieces keep their shape with no deformation signals and apparently they have no defects. This is a good indicative of feedstock homogenisation, good injection and proper further binder elimination stages.

5. Discussion

Classical mixing theory attempts to explain how the torque required to mix a sample is affected by increased solid loading. A model with spherical particles is commonly used to describe the different situations that can occur during mixing of the feedstock components. As the solid loading increases, the particles are more closely packed and there is less inter-particle space occupied by the binder. This normally leads to an increased mixing torque. For PIM feedstocks with spherical or round-shaped powders, the critical powder volume content means that particles are tightly packed touching ones each other by contact points. The binder fills all voids between particles but it does not form a coating separating particles. At the critical solid loading, under classical torque behaviour, the mixing torque increases significantly and becomes erratic due to inter-particle friction. Once the critical point is surpassed, there is no longer enough binder to cover the particles and the capacity of the binder to trap the powder particles diminishes resulting in a reduction of the mixing torque. The feedstock density is also reduced due to void formation in regions that the binder is unable to fill. An optimal solid loading is defined as the ratio of powder to binder near the critical solid loading level in which the particles are tightly packed but there is still sufficient binder to coat them.

For irregularly shaped particles an equivalent particle diameter could be assessed. However, the ability of classical theory to describe non-conventional PIM powders is limited. Increased surface contact is possible with irregularly shaped particles potentially increasing the interparticle friction drastically. A critical situation can also arise without actual particle contact if the particle movement is blocked by severe packing. This can take place even when the particles have a fine coating of binder, which usually acts as a lubricant, if the powder geometry does not allow proper powder flow.

Fig. 12 attempts to visually explain this issue. Fig. 12A describes a typical situation in which there is an excess of binder. Particles can move with relative freedom, even with enough space for rotation. The opposite situation, in which there is an excess of powder, is shown in Fig. 12D with voids coloured black. Fig. 12B represents a high particle packing situation in which binder covers all particles and the particles do not touch; this can be considered optimal solid loading, though the freedom of movement seems to be reduced sufficiently to possibly disallow rotation. The situation presented in Fig. 12C is even more tightly packed than Fig. 12B in which there is evidence of some point contacts, but there is still enough binder to coat the majority of the particles, a critical loading. Situations B and C would presumably result in high mixing torque values, making it difficult to ascertain which of the situations corresponds to the critical. Although particle movement seems to be prohibited, if it happens, it could be explained by the presence of continuous regions with high binder content along a specific direction.

Torque experiments carried out with zircon feedstocks show that a critical situation can occur for solid loadings in which mixing torque stabilises over time. These findings are compared with density measurements and capillary rheology and are reflected in high increases in mixture temperatures and specific processing

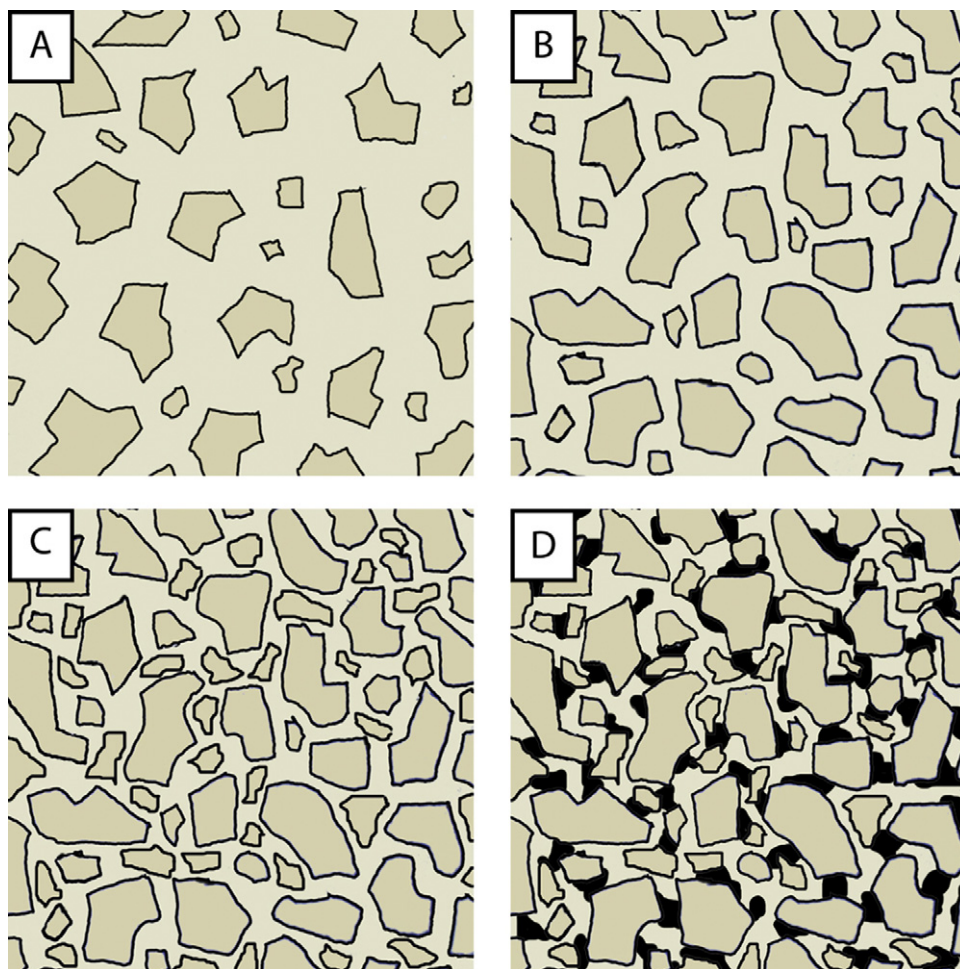


Fig. 12. Models of different situations in loaded binders: (A) excess of binder, (B) optimal load, (C) critical load, (D) excess of powder with black areas representing voids.

energies. The melted feedstock flow could be explained by the existence of continuous binder-rich regions which allow movement in certain directions without particle friction, which would lead to torque values lower than expected and stabilisation of the mixing torque at the CPVC. This idea has been proposed by others previously²² and is known as the slip band theory.

This theory could be consistent with Aggarwal et al.⁷ findings. In their work they noticed abnormal torque behaviour with an increase in the torque observed when the solid loading was increased in the feedstock; however, the torque unexpectedly stabilised rather than become erratic for solid loadings corresponding to the CPVC value. This was attributed to a lack of point contacts between particles or what could be related with the slip bands. Nevertheless, the number of particle contacts increases with an increase of the solid loading and is evinced by the rise in feedstock temperature during torque measurements.

6. Conclusions

Facing the task of evaluating the feedstock mixing behaviour of unconventional PIM powders requires special care in the interpretation of results. A combination of different techniques becomes necessary to make a reliable evaluation. Torque

rheology experiments provide evidence of the physical changes in the feedstocks during the mixing process.

Monitoring of feedstock temperature can be a powerful tool for interpretation of the mixing mechanism and for determining the optimal mixing parameters. A direct relation between torque and feedstock temperature was revealed by taking into account the level of particle friction, which causes these parameters to rise or fall together. The use of totalised torque curves allows evaluation of energy dissipation during processing that is consistent with the temperature results. The level of temperature rise could be abrupt for loadings near the CPVC composition, which was determined to be between 60 and 62.5 vol.%. These results were contrasted with capillary rheology and density measurements. The optimum solid loading resulted to be 57.5 vol.% which presents the best rheological conditions and an absence of agglomerates due to effective mixing. A complete PIM process was successfully carried out for an optimum solid loading feedstock.

Acknowledgements

The authors would like to acknowledge the companies GUZMÁN GLOBAL S.L and ALFA MIMTech for their support

and partnership in the project IPT-2011-0931-020000 granted from the Spanish Ministry of the Economy and Competitiveness and the European Funds for Regional Development (FEDER). They would also kindly thank the Applied Mechanics Department of FEMTO-ST Institute and the ENSMM (Besançon, France) where some of the experimental works were performed. The suggestions and technical support of T. Barriere and G. Michele were much appreciated.

References

1. German RM, Bose A. *Injection molding of metal and ceramics*. Metal Powder Industries Federation; 1997.
2. Mutsuddy BC, Ford RG. *Ceramic injection molding*. UK: Chapman and Hall; 1995.
3. Suri P, Atre SV, German RM, Souza JP. Effect of mixing on the rheology and particle characteristics of tungsten-based powder injection molding feedstock. *Mater Sci Eng* 2003;**A356**:337–44.
4. Contreras JM, Jiménez-Morales A, Torralba JM. Experimental and theoretical methods for optimal solid loading calculation in MIM feedstocks fabricated from powders with different particle characteristics. *Powder Metall* 2010;**53**(1):34–40.
5. Supati R, Loh NH, Khor KA, Tor SB. Mixing and characterization of feedstock for powder injection molding. *Mater Lett* 2000;**46**:109–14.
6. Schramm G. *A practical approach to rheology and rheometry*. 2nd ed. Germany: Thermoelectron; 2004.
7. Aggarwal G, Park SJ, Smid I. Development of niobium powder injection molding. Part I: feedstock and injection molding. *Int J Refract Met Hard Mater* 2006;**24**:253–62.
8. Barreiros FM, Vieira MT. PIM of non-conventional particles. *Ceram Int* 2006;**32**:297–302.
9. Checot-Moinard D, Rigollet C, Lourdin P. Powder injection moulding PIM of feedstock based on hydrosoluble binder and submicronic powder to manufacture parts having micro-details. *Powder Technol* 2011;**208**:472–9.
10. Agote I, Odriazala A, Gutiérrez M, Santamaría A, Quintanilla J, Coupelle P, Soares J. Rheological study of waste porcelain feedstocks for injection moulding. *J Eur Ceram Soc* 2001;**21**:2843–53.
11. Vieira MT, Catarino L, Oliveira M, Sousa J, Torralba JM, Cambronero LEG, Gonzalez-Mesonos FL, Victoria A. Optimization of the sintering process of raw material wastes. *J Mater Process Technol* 1999;**92–93**: 97–101.
12. Bernardo E, Hidalgo J, Jiménez-Morales A, Torralba JM. Feedstock development for powder injection moulding of zirconium silicate. *PIM International* 2012;**6**:64–7.
13. Cheremisinoff NP. *Product design and testing of polymeric materials*. USA: Marcel Dekker; 1990.
14. Abu-Orf M, Örmeci B. *A new tool for measuring biosolids floc strength*. USA: IWA, Publishing; 2004.
15. Escocio V, Altstadt V, Visconte L, de Carvalho M, Nunes R. TPU/mica composites prepared in torque rheometer: processability, mechanical properties and morphology. *Chem Chem Technol* 2011;**5**(2):191–5.
16. Lapa VLC, Visconte LLY, Affonso JES, Nunes RCR. Aluminium hydroxide and carbon black filled NBR/PVC composites – vulcanization and processability studies. *Polym Test* 2002;**21**:443–7.
17. Hausnerova B. Rheological characterization of powder injection molding compounds. *Polimery* 2010;**50**(1):3–11.
18. Kurzbeck S, Kaschta J, Munstedt H. Rheological behaviour of a filled wax system. *Rheol Acta* 1996;**35**:446–57.
19. Allaire F, Marple BR, Boulanger J. Injection-molding of submicrometer zirconia – blend formulation and rheology. *Ceram Int* 1994;**20**(5): 319–25.
20. Weir FE. Moldability of plastics base on melt rheology. *Soc Plast Eng Trans* 1963;**3**:32–6.
21. Li Y, Huang B, Qu X. Viscosity and melt rheology of metal injection moulding feedstocks. *Powder Metall* 1999;**42**(1):86–90.
22. Chuankrerkkul N, Messer PF, Davies HA. Flow and void formation in PIM feedstocks made with PEG/PMMA binders. Part 2: slip band theory. *Powder Metall* 2008;**51**:72–7.